Ambiguity Resolution of Two Conformal Leaky-Wave Antennas via Deep Learning

A. Gil-Martínez*, J. Perez-Valero*, J. A. López-Pastor†, J. L. Gómez-Tornero‡, A. Skarmeta-Gómez*

*Department of Information and Communications Engineering, University of Murcia, 30100 Murcia, Spain

†Department of Engineering and Applied Technologies, University Center of Defense, San Javier Air Force Base, 30729, Spain

‡Department of Information and Communications Technologies, Technical University of Cartagena, 30202 Cartagena, Spain

Abstract—Ambiguities in direction-of-arrival (DoA) estimation introduces significant challenges in wireless communication systems, particularly in applications requiring precise localization and sensing. These ambiguities can lead to misinterpretation of signal origins, severely impacting the performance and localization of systems such as Wireless Body Area Networks (WBANs) and Internet of Things (IoT) devices. In this paper, we investigate the ambiguities in an array of two symmetric conformal leaky-wave antenna (LWA) system, which, while offering enhanced field-of-view coverage, introduces complexities in resolving directional ambiguities. To address this issue, we propose a novel ambiguity resolution model based on a Long Short-Term Memory (LSTM) network. Our proposed LSTM-based approach achieves an accuracy of 99.99% in resolving ambiguities in comparison with other state of the art techniques. This advancement not only strengthens the reliability of conformal LWA systems but also lays the foundation for more robust and precise localization in wireless scenarios.

Index Terms—Conformal antenna, ambiguity resolution, recurrent neural networks.

I. Introduction

Flexible antennas are expected to become key enablers in the Internet of Things (IoT) ecosystem due to their ability to conform to a wide variety of deployment surfaces [1]. Given their versatility, conformal antennas are particularly well-suited for IoT wireless systems, specifically in Wireless Personal Area Networks (WPANs) and Wireless Body Area Networks (WBANs) [2]. These networks need flexible antennas that maintain performance while conforming to surfaces like the human body. Furthermore, managing electromagnetic coupling under surface deformation remains a major challenge in conformal antenna design. In addition, the electromagnetic distortion caused by the curvature of the antenna material generates ambiguities in Direction of Arrival (DoA) systems, adding a further degree of complexity when shaped antennas are implemented in IoT localization applications.

In this paper, we introduce the design of a conformal microstrip leaky-wave antenna (MLWA) using the Bluetooth Low Energy (BLE) frequency band and recurrent neural networks (RNN) for DoA ambiguity mitigation. Such ambiguities commonly appear as a multiple solutions that solve the DoA problem, e. g. symmetric peaks at $\pm\theta$ in the DoA algorithm. MLWAs present advanced functionalities, such as low power consumption, reduced design complexity and passive beam scanning [3]. Thus, MLWAs have recently become popular due
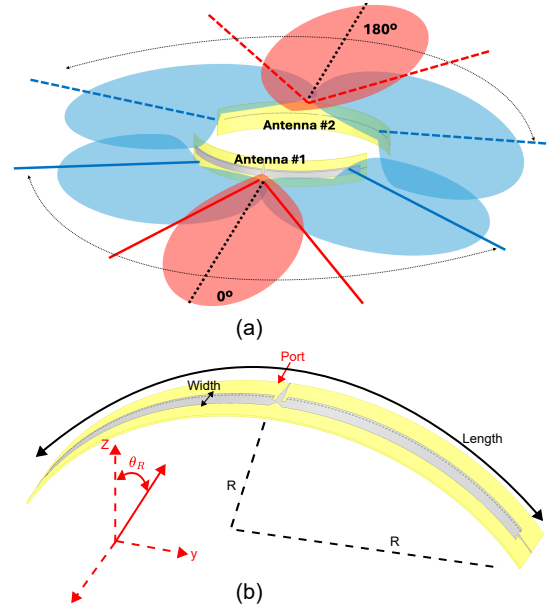

Fig. 1: (a) Schematic illustration of full azimuthal scanning using two conformal leaky-wave antennas (LWAs). (b) Design schematic of the conformal LWA structure.

to their excellent performance in DoA applications, including Wi-Fi [4] and RFID [5]. Compared to other antenna technologies, MLWAs offer straightforward feeding mechanisms, frequency-dependent beam scanning, low profile structure, and simple antenna design. Moreover, MLWAs can be easily adapted to flexible substrates, further enhancing their applicability in wearable and conformal antenna applications.

Recently, the research community has shown significant interest in addressing ambiguity resolution in both outdoor and indoor scenarios using different technologies. For instance, [6], [7] explore ambiguity resolution in Global Navigation Satellite Systems (GNSS) through different antenna configurations. Artificial intelligence has been also extensively explored in the literature for both indoor and outdoor positioning. For example, a comprehensive systematic review [8] outlines various AI techniques—such as convolutional neural networks (CNNs), recurrent neural networks (RNNs), and traditional machine learning methods—applied to indoor localization. In

[9], the authors propose an algorithm that combines multi-sensor fingerprinting with deep learning for improved indoor positioning. Similarly, [10] presents a machine learning approach utilizing a random forest classifier to estimate a user's or object's location based on RSSI fingerprinting. Additionally, [11] introduces a radar-semantics-modeled long short-term memory (LSTM) algorithm for enhanced positioning accuracy.

The studies most relevant to our work are [12], [13] and [14]. In [12], authors propose the use of flat-top broad beams to mitigate DoA ambiguities in amplitude-monopulse systems. Similarly, [13] assesses three techniques for efficiently utilizing received signals from both ports of 1-D frequency beam scanning LWAs with the MUSIC algorithm. Finally, [14] proposes the combination of amplitude and phase comparison techniques to partially resolve the ambiguities in multibeam antenna systems.

In the context of artificial intelligence, [15] proposes a RRN-based ambiguity resolution method to estimate the precise attitude of the GNSS sensor matrix. However, none of these works explore the synergy between deep learning and LWAs to resolve amplitude ambiguities for both indoor and outdoor localization. Our proposal complements prior works by leveraging deep learning techniques to enhance ambiguity resolution in LWAs, unlocking new possibilities for accurate and robust localization in diverse environments.

In a nutshell, the main contributions of the paper are as follows:

- We design two tapered conformal MLWAs for full-azimuthal scanning (360°) as shown in Fig. 1(a).
- We combine deep learning models with amplitude monopulse techniques to address the inherent ambiguities in DoA estimation.
- We compare our proposed LSTM-based ambiguity resolution model with state of the art methods, achieving 99.998% accuracy in mitigating false detections. The implemented models are tested with simulated data.

The rest of this paper is organized as follows. In Section II we explain the conformal tapered MLWA design to apply amplitude monopulse DoA techniques. In Section III we show the full azimuthal radiation patterns applying amplitude monopulse. In Section IV we present the LSTM model for ambiguity resolution. In Section V we evaluate the accuracy of the LSTM model and compare against other state of the art methods. Finally, in Section VI, we conclude the paper.

II. ANTENNA DESIGN

The implementation of rectilinear MLWAs generating directive frequency-scanned beams within a defined field-of-view (FoV) using a limited bandwidth has been extensively explored in recent years [3], [5]. In particular, the half-width microstrip (HWM) LWA[1] presents a remarkably simple structure, consisting of a metallic strip of length L and width

---

[1]The antenna design and simulations are performed using HFSS (High Frequency Structure Simulator) software.

W, printed on a grounded substrate with permittivity ϵ_r and thickness H.

The strip width W and the substrate permittivity ϵ_r determine the frequency beam-scanning response $\theta(f)$, which defines the angular FoV covered within a specified scanning bandwidth ranging from f_1 to f_2. This relationship can be approximated using the following expressions [16]:

$$\sin^2 \theta_r(f) = \epsilon_r - (\frac{c_0}{4fW})^2 \tag{1}$$

$$FoV = \frac{2}{\theta_r(f_2)} \tag{2}$$

while the antenna strip length L_A determines the half-power beamwidth Δ_θ by the next approximate formula:

$$\Delta_\theta = \frac{57c_0}{L_A f \cos \theta_r} \tag{3}$$

where c_0 represents the speed of light. In the case of BLE, the lowest channel frequency is $f_1 = 2.402$ GHz (i.e., channel #37), while the highest channel frequency is $f_2 = 2.48$ GHz (i.e., channel #39) [3]. As detailed in [3], [4], the dielectric substrate selection is a critical factor when defining the frequency beam-scanning response $\theta(f)$ of the HWM LWA, as described by equation (1).

To reduce the number of ports from two to one while maintaining a wide angular FoV, a center-fed HWM-LWA has been investigated. The simulated schematic of this antenna is depicted in Fig. 1(b). In this design, the feeding port is centrally positioned along the radiating strip, with two dummy adapted ports placed at each end to minimize reflections. Two antenna designs have been analyzed using the RT/Duroid 6010 substrate, which features a permittivity of $\epsilon_r = 10.2$ and a thickness of $H = 1.27$ mm. This choice enables the maximization of the FoV within the BLE bandwidth. HWM LWAs have been extensively employed for indoor localization [4], [5] due to their structural simplicity and their capability to generate mirrored frequency-scanned beams in different spatial directions by merely altering the frequency.

In addition, achieving a wider FoV while maintaining the radiation characteristics of the antenna is highly desirable in localization and sensing applications. However, this goal is often constrained by limitations in substrate materials, as substrates with a permittivity (ϵ_r) higher than 10.2 are difficult to source and significantly complicate both the antenna design and fabrication processes.

To overcome this limitation, we propose increasing the FoV by curving the flexible substrate in a controlled manner using tapering techniques in the same fashion as proposed in [17] and experimentally demonstrated in [18]. Therefore, the curvature-induced defocusing effect is reduced and directive patterns are computed. The curvature radius R of the antenna is controlled using the following expression:
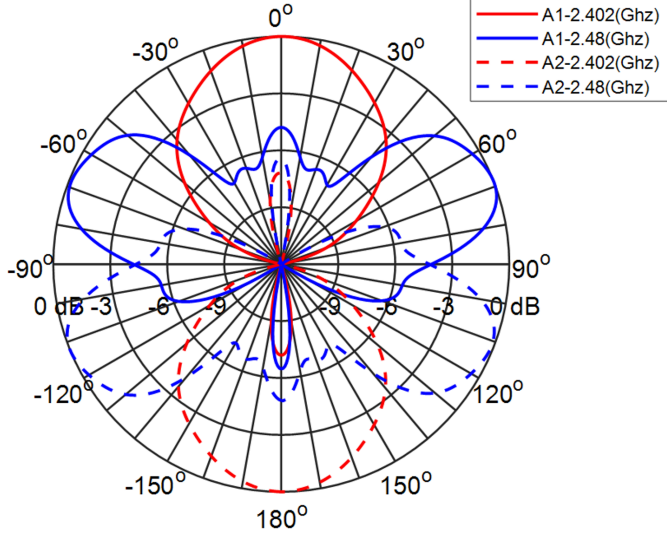
$$R = \frac{\Delta_L}{(2\pi/3)} \tag{4}$$

Fig. 2: Simulated full azimuthal radiation patterns, where red patterns correspond to channel #37 and blue patterns correspond to channel #39.

where Δ_L represents the total antenna length, which includes the metallic strip length L and the microstrip feeding lines $2L$ feed. In this design, the total antenna length is $\Delta_L = 34$ cm, and to achieve a FoV of 180º, the required curvature radius is $R = 16.52$ cm.

The corresponding radiation pattern of the conformal width-tapered HWM-LWA is shown in Fig. 2, noticing the full-azimuthal scanning with only two conformal LWAs and two-ports. However, this configuration introduces ambiguities in mobile device detection, as it becomes impossible to determine whether a device is located at a positive $+\theta$ or negative $-\theta$ angle. To mitigate such ambiguities, several techniques have been proposed in the literature, including the use of broad-beam patterns through multiple ports [12] or the implementation of multibeam LWAs [13].

III. Full azimuthal scanning

We use two conformal LWAs to cover a total FoV of 360º while requiring only two antenna ports. Among all localization algorithms, we select amplitude-monopulse RADAR techniques due to their cost-effective and simple implementation. To apply the over-the-air (OTA) amplitude monopulse algorithm, we compute the monopulse function from the resulting radiation patterns for each pair of frequency-scanned beams in the same fashion as [19]:

$$MF_n = \frac{\Delta_n(\theta)}{\Sigma_n(\theta)} = \frac{P_{n+1} - P_n}{P_{n+1} + P_n} \quad (5)$$

where n is the selected frequency channel for each antenna (corresponding to channel #37 or #39), $\Delta_n(\theta)$ and $\Sigma_n(\theta)$ represent the difference and sum patterns for each pair combination, respectively. Using the proposed full-azimuthal array, a total of three monopulse functions are obtained.

Fig. 3(a) shows the computed monopulse functions for each beam pattern combination while Fig. 2 present the full azimuthal scanning. For example, in Fig. 2, when the red solid beam pointing to 0º is computed using (5) together with its adjacent blue pattern (formed by two main lobes), the resulting red monopulse function is shown in Fig. 3(a). Similarly, by combining the red and blue dashed patterns in Fig. 2, the green monopulse function is derived in Fig. 3(a). Finally, the yellow monopulse function in Fig. 3(a) is obtained by the combination of both blue patterns in Fig. 2, that correspond to the use of f_2 conformal LWA1 and f_2 in the conformal LWA2.

$$MV_n = \frac{RSS_{n+1} - RSS_n}{RSS_{n+1} + RSS_n} \quad (6)$$

To determine the DoA of any incoming signal, the received strength signal (RSS) values measured from both antennas using all the available frequency channels are processed and combined to generate three monopulse values, denoted in Eq. (6). These values are then compared against pre-characterized monopulse functions to estimate the DoA, thus obtaining the estimated angular pseudospectrum (APS). For each RSS, the estimated DoA angle theta is determined by identifying the angle that maximizes the combined inverse error function, as expressed in the following equation (7) [19], [20]:

$$\theta_{est} = max(10log10(\frac{1}{\sqrt{(MF_n(\theta) - MV_n)^2/N}})) \quad (7)$$

Fig. 3(b) illustrates the computed APS for real angles of -20º, +80º and +180º, with red, green and blue solid lines, respectively. As can be noticed for the three proposed APSs, a peak pointing to the real angle is obtained, however, another azimuthaly symmetric peak (ambiguity) is also measured. Therefore, correct estimation of the DoA angle is unfeasible due to the appearance of ambiguities. Generally, the secondary peaks that can be observed in APSs are produced in low SNR or multipath situations, and are typically considered ambiguities, since they result in false detections. In contrast, the false detections in the proposed architecture are caused by the symmetry in the design of the full-azimuthal array and cannot be solved by the monopulse amplitude technique itself. Therefore, in this paper we propose a post-processing step based on recurrent neural networks to reduce the number of ambiguities generated by a conformal symmetric antenna array.

IV. LSTM model description

In this section, we provide a detailed description of the used dataset and LSTM model.

A. Dataset

The dataset[2] used for evaluation comprises 360,000 simulated signal instances, generated using commercial software

[2]The dataset and source code are available at: https://github.com/jpvalero/ambiguity-resolution-with-deep-learning
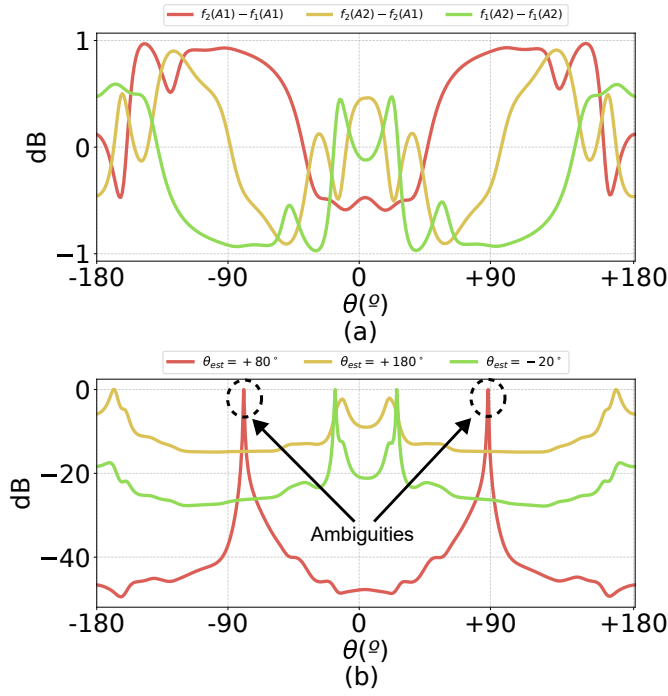
Fig. 3: (a) Computed monopulse functions for different beam pattern combinations; (b) Angular pseudospectrum with directional ambiguities for different angles

such as MATLAB and providing precise azimuthal DoA information. These simulations cover 360 different angles, with 1,000 samples per angle, ensuring comprehensive angular coverage. Each instance is structured as a time series of 1,000 timesteps, with a single feature per timestep, capturing fine-grained temporal variations in the signal.

B. Model Architecture

The proposed deep learning model is based on a Long Short-Term Memory (LSTM) network designed to classify signals as ambiguous or non-ambiguous. We depict the architecture of the LSTM model in Fig. 4. The first LSTM layer has 128 memory cells, returns the full sequence, and is followed by batch normalization and 40% dropout to improve training stability and reduce overfitting. The second LSTM layer has 64 memory cells and returns only the final output, summarizing temporal dependencies into a single feature vector. The classification layer consists of a dense layer with 32 neurons (ReLU activation), followed by a sigmoid-activated output neuron for binary classification. We summarize the main parameters of the architecture in Table. I. The model is trained using the Adam optimizer with a 0.001 learning rate, for 20 epochs, with a batch size of 32 samples, and validated with 20% of the dataset reserved for testing. All experiments were conducted on an AMD Ryzen 5 7530U processor (6 cores, 12 threads) running at a base frequency of 2 GHz, with 16 GB of RAM.

Hyper-Parameter	Value
Learning Rate	0.001
Dropout	0.4
Activation function	sigmoid (output)
Optimizer	adam
Epoch	20
Batch size	32
Loss function	binary_crossentropy

TABLE I: Hyper-parameters of the experiments.

C. Implementation details

The LSTM model is implemented using TensorFlow [21], which is a data-flow graph-based numerical computation library developed by Google. Leveraging TensorFlow's Python, the trained model can be seamlessly integrated into software-defined radio (SDR) frameworks. This compatibility allows the model to be deployed e.g., as a reusable processing block within GNU Radio's signal processing flowgraphs, enabling real-time ambiguity resolution with minimal latency. Once trained, the model can be directly interfaced with hardware front-ends supporting GNU Radio, such as low-cost SDRs (e.g., USRP or RTL-SDR), making it practical for IoT and WBAN applications.

V. PERFORMANCE EVALUATION

In this section, we evaluate the performance of the proposed LSTM model described in Section IV.

A. Model Classification Accuracy and Losses

In Fig. 5, we depict the classification accuracy and loss trends over 10 different iterations of training, demonstrating the stability and consistency of the proposed model. For instance, the accuracy curve in Fig. 5(b) shows a steady increase across all iterations. The final validation accuracy converges at approximately 99,9%, indicating that the model effectively captures the underlying patterns in the dataset.

The loss curves in Fig. 5(a) consistently decreases across all 10 training iterations, indicating effective model learning and convergence. As training progresses, the rate of decrease slows down, and the training loss stabilizes after approximately 4 epochs, suggesting that the model has reached its optimal learning capacity without overfitting. The consistency of these trends over multiple runs confirms the reliability of the training process, reducing concerns about instability or excessive sensitivity to specific data samples.

B. Results

We illustrate in Fig. 6 the confusion matrix for a subset of angles $\theta = \{-180°, -177°, -1°, 180°\}$, providing insight into the classification performance of our model. The confusion matrix summarizes the correct and false predictions. Fig. 6(a) presents the classification results for $\theta = -180°$, where our model perfectly distinguishes between non-ambiguous and ambiguous signals. Note that a diagonal

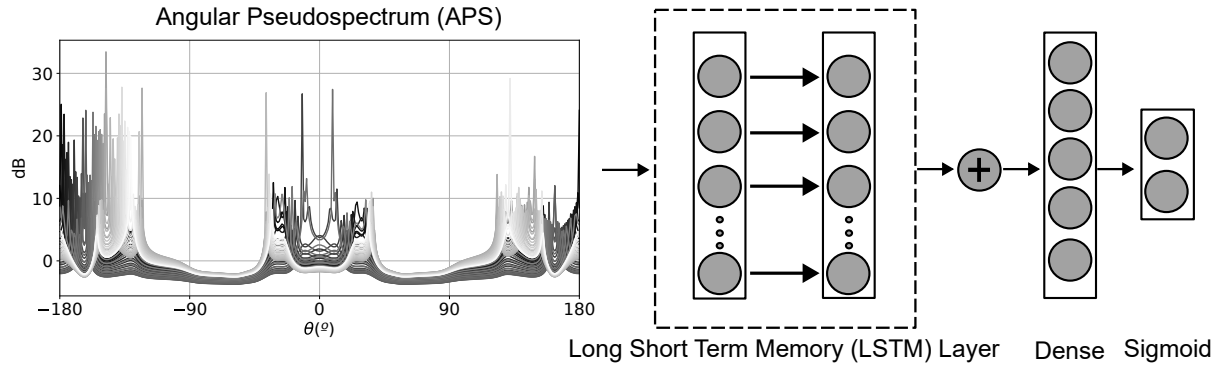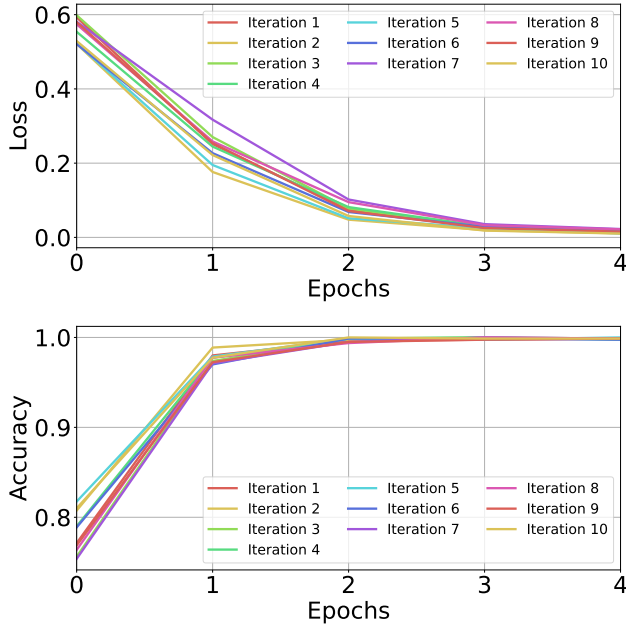Fig. 4: LSTM model architecture.

C. Comparison

Finally, to demonstrate the enhanced localization performance by combining amplitude monopulse techniques with an LSTM network, we compare the proposed LSTM-based model against four different state-of-the-art ambiguity resolution methods (see Table. II). The metrics used for comparison are the Mean Absolute Error (MAE), Root Mean Square Error (RMSE) and accuracy. Firstly, the amplitude monopulse technique [20] is computed using the limiting frequency channels within the three available channels in the BLE 2.4 GHz band (#37 and #39). As demonstrated in previous sections, by simply using two conformal LWAs and two frequency channels, a full-azimuthal scanning is achieved. However, as observed in Table II, the obtained MAE and RMSE metrics are above 35º and 40º, due to ambiguities. Using multiple frequency channels with localization algorithms has recently been proposed as a technique to reduce ambiguities [13], because extra channels provide additional spatial-frequency information. However, since the BLE protocol has only three available frequency channels (#37, #38 and #39), this technique does not significantly reduce ambiguities in the proposed system. As observed in Table II, the MAE and RMSE have decreased, but they remain above 30° in both cases. Given the complexity of the problem, we compare our LSTM-based approach with two more sophisticated methods. More specifically, we compare our method with a Deep Belief Network (DBN) inspired from [9]. The DBN is a type of generative model made up of multiple layers of Restricted Boltzmann Machines (RBMs) followed by a softmax layer for classification. Additionally, we compare our method agains a Random Forest module such as [10] adapted to meet our problem formulation. Similar results are obtained using DBN and random forest, reducing the MAE and RMSE to 0.4º and 1.8º with accuracy above 99.8%. Lastly, when the amplitude monopulse technique is computed and combined with an LSTM network to classify and correct the ambiguities, the accuracy is increased up to 99.99% and localization error is reduced to 0.3º and 1.7º for MAE and RMSE, respectively. Since the DBN, Random Forest, and LSTM all exhibit similarly high performance, any of them could effectively resolve the ambiguities. The optimal choice depends on the target application, as the parameterization of
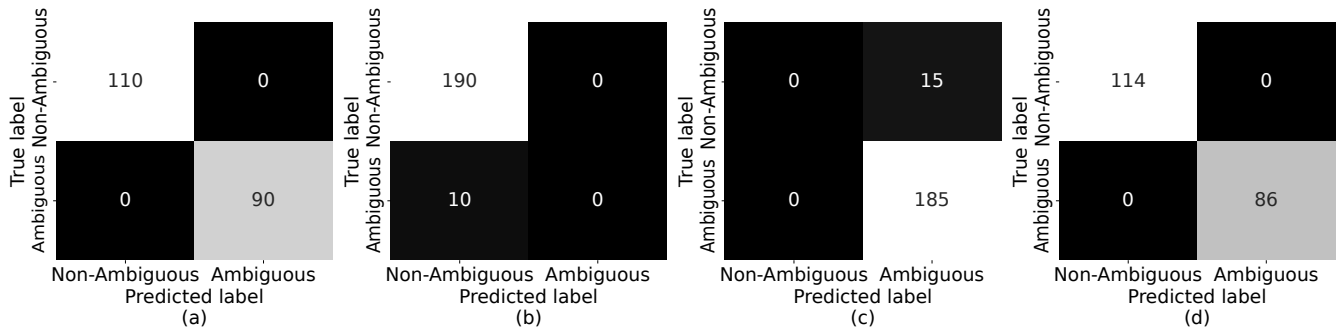

Fig. 5: Training performance of the LSTM-based ambiguity resolution model over 10 independent runs, where (a) shows the loss curves demonstrating consistent convergence, and (b) represents the accuracy trends highlighting stable and reliable learning across iterations.

confusion matrix indicates a 100% success rate. Similarly, Fig. 6(b) shows the classification results for $\theta = -177°$, where our model misclassifies 10 ambiguous signals as non-ambiguous, resulting in a success rate of 94.73%. Additionally, Fig. 6(c) shows the classification results for $\theta = -1°$ where our model misclassifies 15 non-ambiguous signals as ambiguous, resulting in a success rate of 92.10%. Finally, Fig. 6(d) presents the classification results for $\theta = 180°$, where our model perfectly distinguishes between non-ambiguous and ambiguous signals, achieving a 100% success rate. We repeat this process for the remaining θ angles, achieving an overall classification accuracy of 99.998%.

Fig. 6: Confusion matrices for three different DoA angles: (a) $\theta = -180°$, (b) $\theta = -177°$, (c) $\theta = -1°$, (d) $\theta = 180°$

each method influences the trade-off between generalization capability and computational efficiency.

In terms of the training time, the LSTM model has a significantly longer training time compared to Random Forest and Deep Belief Networks due to its sequential processing of time steps, complex gating mechanisms (input, forget, output gates), and backpropagation through time (BPTT), which limit parallelization. In contrast, Random Forests train quickly by building independent decision trees in parallel, while DBNs use efficient feedforward operations without recurrence.

VI. CONCLUSION AND FUTURE WORK

In contrast to traditional ambiguity resolution methods in DoA estimation, this paper introduces a lightweight, LSTM-based deep learning model to resolve inherent ambiguities in conformal LWA systems. By integrating amplitude monopulse techniques with a recurrent neural network, our approach achieves 99.99% accuracy in distinguishing true signal origins from symmetric false detections, despite the antenna array's full-azimuthal symmetry. Through extensive evaluation using simulated data from the designed antenna, we evaluate the performance of the proposed LSTM-based model against other state of the art methods, establishing it as a practical solution for cost- and energy-efficient solution for precise localization in next-generation wireless sensing and communication systems.

As part of our ongoing and future work, we are exploring several key directions to enhance the robustness and applicability of our method. First, we aim to transition from simulated data to real-world scenarios. This transition may arise some challenges such as multipath propagation, signal noise, and the influence of surrounding materials on antenna performance. Addressing these issues will be key to validate the generalization capability of our model. Second, although our approach demonstrates very high classification accuracy (99.998%) compared to baselines such as Random Forest and DBN, we recognize the risk of overfitting inherent in such results when relying solely on synthetic data. To address this, we will include experimental validation using physical antenna prototypes and real measurement campaigns to assess the method's performance under realistic conditions.

REFERENCES

[1] H. Huang, "Flexible wireless antenna sensor: A review," *IEEE Sensors J.*, vol. 13, no. 10, pp. 3865–3872, 2013.

[2] D. M. G. Preethichandra, L. Piyathilaka, U. Izhar, R. Samarasinghe, and L. C. De Silva, "Wireless body area networks and their applications—a review," *IEEE Access*, vol. 11, pp. 9202–9220, 2023.

[3] J. L. Gómez-Tornero, *Smart Leaky-Wave Antennas for Iridescent IoT Wireless Networks*, 2022, pp. 119–181.

[4] A. Gil-Martinez, J. A. López-Pastor, M. Poveda-Garcia, A. Algaba-Brazález, D. Cañete-Rebenaque, and J. L. Gómez-Tornero, "Monopulse leaky wave antennas for rssi-based direction finding in wireless local area networks," *IEEE Trans. Antennas Propag.*, vol. 71, no. 11, pp. 8602–8615, 2023.

[5] A. Gil-Martínez, M. Poveda-García, J. García-Fernández, M. M. Campo-Valera, D. Cañete-Rebenaque, and J. L. G. Tornero, "Direction finding of rfid tags in uhf band using a passive beam-scanning leaky-wave antenna," *IEEE Journal of Radio Frequency Identification*, vol. 6, pp. 552–563, 2022.

[6] B. Li and P. J. Teunissen, "Gnss antenna array-aided cors ambiguity resolution," *Journal of geodesy*, vol. 88, no. 4, pp. 363–376, 2014.

[7] T. Ballal and C. J. Bleakley, "Gnss instantaneous ambiguity resolution and attitude determination exploiting the receiver antenna configuration," *IEEE Transactions on Aerospace and Electronic Systems*, vol. 50, no. 3, pp. 2061–2069, 2014.

[8] V. Bellavista-Parent, J. Torres-Sospedra, and A. Perez-Navarro, "New trends in indoor positioning based on wifi and machine learning: A systematic review," in *2021 International Conference on Indoor Positioning and Indoor Navigation (IPIN)*, 2021, pp. 1–8.

[9] X. Gan, B. Yu, L. Huang, and Y. Li, "Deep learning for weights training and indoor positioning using multi-sensor fingerprint," in *2017 International Conference on Indoor Positioning and Indoor Navigation (IPIN)*, 2017, pp. 1–7.

[10] E. Jedari, Z. Wu, R. Rashidzadeh, and M. Saif, "Wi-fi based indoor location positioning employing random forest classifier," in *2015 International Conference on Indoor Positioning and Indoor Navigation (IPIN)*, 2015, pp. 1–5.

Method	MAE (°)	RMSE (°)	Accuracy (%)	Training time (sec)
Amplitude Monopulse [20]	35	42	-*	-
Multifrequency amplitude monopulse [13]	33.1	39.8	-*	-
Deep Belief Network (DBN) [9]	0.4	1.8	99.79	2.06
Random Forest Classifier [10]	0.4	1.8	99.85	0.01
LSTM-based model (our proposal)	0.3	1.7	99.99	85.42

* Note that accuracy is not reported for amplitude monopulse and multifrequency amplitude monopulse, as these methods cannot resolve angular ambiguities.

TABLE II: Performance comparison of state-of-the-art methods.

[11] C. He, L. Zhang, S. Wei, and Y. Fang, "Multifunction radar working mode recognition with unsupervised hierarchical modeling and functional semantics embedding based lstm," *IEEE Sensors J.*, vol. 24, no. 14, pp. 22 698–22 710, 2024.

[12] M. Poveda-García and J. L. Gómez-Tornero, "Ambiguity resolution in amplitude-monopulse systems using broad-beam patterns," *IEEE Antennas and Wireless Propagation Letters*, vol. 20, no. 4, pp. 503–507, 2021.

[13] J. Sarrazin and G. Valerio, "Direction-of-arrival ambiguities mitigation in multibeam leaky-wave antennas," in *2024 18th European Conference on Antennas and Propagation (EuCAP)*. IEEE, 2024, pp. 1–5.

[14] M. Hutar, J. López-Pastor, A. Gil-Martínez, P. Brida, and J. Gómez-Tornero, "Combined phase-difference and amplitude-comparison technique for wi-fi direction-finding with high angular sensitivity and ambiguity mitigation in a wide field of view," *Results in Engineering*, p. 104711, 2025.

[15] R. de Celis, P. Solano-Lopez, J. Barroso, and L. Cadarso, "Neural network-based ambiguity resolution for precise attitude estimation with gnss sensors," *IEEE Trans. Aerospace Electr. Syst.*, vol. 60, no. 5, pp. 6702–6716, 2024.

[16] A. A. Oliner, "Leakage from higher modes on microstrip line with application to antennas," *Radio Science*, vol. 22, no. 06, pp. 907–912, 1987.

[17] J. L. Gomez-Tornero, "Analysis and design of conformal tapered leaky-wave antennas," *IEEE Antennas Wireless Propag. Lett.*, vol. 10, pp. 1068–1071, 2011.

[18] A. J. Martinez-Ros, J. L. Gómez-Tornero, and G. Goussetis, "Conformal tapered substrate integrated waveguide leaky-wave antenna," *IEEE Transactions on Antennas and Propagation*, vol. 62, no. 12, pp. 5983–5991, 2014.

[19] D. Barton and S. Sherman, *Monopulse Principles and Techniques, Second Edition*, 2011.

[20] E. Mosca, "Angle Estimation in Amplitude Comparison Monopulse Systems," *IEEE Trans. Aerospace Electr. Syst.*, vol. AES-5, no. 2, pp. 205–212, 1969.

[21] M. Abadi, A. Agarwal, P. Barham, E. Brevdo, Z. Chen, C. Citro, G. S. Corrado, A. Davis, J. Dean, M. Devin *et al.*, "Tensorflow: Large-scale machine learning on heterogeneous distributed systems," *arXiv preprint arXiv:1603.04467*, 2016.